Low-cycle fatigue of an aluminum alloy plated with multi-layered deposits

Ya. B. UNIGOVSKI*, A. GRINBERG, E. GERAFI, E. M. GUTMAN, S. MOISA
Ben-Gurion University of the Negev, Department of Materials Engineering, Beer-Sheva, Israel

Low-cycle fatigue (LCF) in engineering structures is caused by a relatively low-frequency strain cycling or thermal cycling. Regardless of the fact that it is much more dangerous than high-cycle fatigue, it has not been studied enough. Coated aluminum alloys are widely used in aerospace and transportation industries, mostly because of their high toughness and strength-weight ratio and improved surface properties. The effect of one-, two- and three-layer coatings, including an inner electroless nickel layer and, additionally, electrodeposited nickel, gold and silver, on the LCF behavior of 1.6-mm-thick 6061-T6 Al alloy was studied in a strain-controlled purely bending mode. The lifetime of the coated alloy drastically decreases as compared to the substrate. The incipient cracks were revealed, first of all, in the electroless nickel layer and in the substrate close to its surface.

(Received March 25, 2013; accepted July 11, 2013)

Keywords: Low-cycle fatigue, Coated aluminum alloy, Deposit thickness

1. Introduction

It is well-known that coated Al alloys often have a relatively low resistance to cycling load, especially, in heavily-loaded parts [1-3]. For example, the coating brittleness and the cracks induced during anodizing are among the factors which affect the fatigue strength of hard anodized components [2, 3]. If the deposit is relatively ductile, e.g., consists of a cobalt-chromium alloy and particles of tungsten carbide, the coating improved the fatigue life of AA6063-T6 aluminum alloy [4].

Electroless nickel (EN) is an engineering coating, normally used because of its excellent corrosion and wear resistance. Chemical and physical properties of the deposit vary primarily with phosphorus content and subsequent heat treatment [1, 5]. The results obtained for 7075-T6 [6] and 2618-T61 [7] aluminum alloys coated with an EN deposit show that the coating can give rise to a significant improvement in the fatigue performance of the substrate at medium and low stresses. This improvement was associated with a higher strength of the coating as compared to the substrate and with the development of compressive residual stresses in the coating during the deposition.

All abovementioned literature data demonstrating the fatigue behavior of coated alloys relate to the stress-life method, which works well if only elastic stresses and strains are present. However, most coated components may appear to have nominally cyclic elastic stresses, but various stress concentrators, such as microcracks, notches, welds, etc., present in the component may result in local cyclic plastic deformation. Under these conditions, the local strain as the governing fatigue parameter (the local strain-life method) is much more effective in predicting the fatigue life of a component. In engineering applications, relatively low-frequency strain cycling as a consequence, e.g., of start and stop operations, generates low-cycle fatigue (LCF) failure.

In the literature, there are no reported studies with respect to the LCF behavior of Al alloys plated with a single electroless Ni, and, especially, with multi-layered deposits. In the present investigation, the effect of a single layer and multi-layered coatings on the LCF behavior of a 6061-T6 alloy was studied.

2. Experimental

Solutionized and artificially aged 6061-T6 aluminum alloy consists of, wt.%: 0.4 - 0.8 Si, ≤0.7 Fe, 0.15 - 0.40 Cu, ≤0.15 Mn, 0.8 - 1.2 Mg, 0.04 - 0.35 Cr, ≤0.15 Ti, ≤0.25 Zn, other elements ≤0.05% each, 0.15% total, 95.85 – 98.56 Al. Coupons of this alloy with the dimensions of 110 x 25 x 1.6 mm were coated with a single 12- μm or 26- μm-thick layer of electroless nickel (sets 2 and 3, respectively, Table 1). These layers were deposited on the alloy surface in accordance with ASTM B733 Type V, SC2/SC3. To increase the adhesion of electroless nickel to the aluminum alloy surface, heat treatment at 180^{o}C during one hour was performed after the coupon plating process. Two-layered deposits include an inner 12- μm or 26- μm-thick EN and an outer 3-4- μm-thick electrodeposited Ni layer (EDN) performed in accordance with the standard SAE AMS 2424F-2010 in a nickel sulfamate bath (Table 1). It possesses the lowest internal stress as compared to EN plating.

As represented in Table 1, three-layered coatings have an outer layer of silver (set 6) or gold (set 7) deposited in accordance with ASTM B700 Type 1 Grade A Class N

(thickness class 10μm) or ASTM B488 Type 1 Grade C Class 0.1μm, respectively. Coatings of silver are usually employed for solderable surfaces, electrical contact characteristics, special reflectivity, etc. Electrodeposited gold coatings have high corrosion and tarnish resistance, solderability, infrared reflectivity, etc.

The specimens with the gauge width and length of 10 and 32 mm, respectively, were tested on a Model IP-2 pure bending fatigue machine with the capacity of around 50 Nm in a strain-controlled loading mode at the strain ratio $R = \varepsilon_{min}/\varepsilon_{max} = 0.1$, where ε_{min} and ε_{max} are the minimum and maximum values of the total strain, respectively. The scheme of the LCF test and a view of the sample deflection measurement are given in Ref. [8]. The sine-wave input form with the frequency of 0.4 Hz was used. The force response of the samples during the LCF tests was monitored by the Model 614 Tedea load cell with the loading range of 0 - 2,000 N and a special USB 9237 card (National Instruments Co.) and recorded using LabVIEW program.

Table 1. The outer deposit kind, thickness, roughness (R_a) and Vickers microhardness (VH) as compared to those of the substrate.

The layer	**Kind of a deposit, thickness [μm] and surface properties for sets 1 - 7 *)**						
	1	**2**	**3**	**4**	**5**	**6**	**7**
1	-	12 (EN)	26 (EN)	12 (EN)	26 (EN)	12 (EN)	26 (EN)
2	-	-	-	4 (EDN)	3 (EDN)	4 (EDN)	3 (EDN)
3	-	-	-	-	-	3 (Ag)	0.2 (Au)
R_a, μm	1.98±0.54	0.75±0.20	0.82±0.27	0.91±0.42	0.82±0.37	1.22±0.47	0.82±0.31
HV, GPa	1.05±0.06	4.91±0.09	5.31±0.10	1.94±0.07	1.94±0.07	0.29±0.01	-

***)** EN and EDN denote electroless- and electrodeposited nickel coatings, respectively; Ag and Au are silver and gold coatings, e.g., the set 6 consists of three deposits on the Al alloy substrate: an inner 12-μm EN layer; an intermediate 4-μm EDN layer and an outer 3-μm silver layer.

Three maximum total strains were used in fatigue tests, ($x10^{-2}$): 0.68±0.03; 0.88±0.08 and 1.37±0.12 corresponding to the plastic strain amplitudes $\Delta\varepsilon_{pl}$ amounting to around 0.003, 0.005 and 0.010, respectively. Here the $\Delta\varepsilon_{pl}$ was calculated as a difference between the maximum total strain $\Delta\varepsilon_t$ and maximum elastic strain $\Delta\varepsilon_e = TYS/E$, where *TYS* and *E* are tensile yield stress and elastic modulus, respectively. The testing environment was air at 25°C ± 2 °C.

The tensile properties of uncoated and coated 6061 alloy were performed using a universal testing machine Zwick-1445 at the test speed of 2.6×10^{-3} s^{-1}. The hardness was measured using a HMV-2 Microhardness Vickers tester with a diamond pyramid under the load of 9.81 N (Al substrate), 0.98 N and 0.49 N (EN, EDN), 0.49 N and 0.25 N (Ag). The surface roughness of the alloy and coatings determined as the center-line average height R_a was measured by a Veeco Dektak 150 surface profilometer. The microscopic evaluation of the samples was performed on an optical microscope Axio Observer.A1m (Karl Zeiss, USA) and a scanning electron microscope JEOL JSM-5600 with 'NORON' energy-dispersive analysis system. The X-ray diffraction of EN deposit was performed by Philips X-ray diffractometer using Cu-K_α radiation.

3. Results and discussion.

3.1. Characterization of substrate and deposits properties

The average surface roughness R_a of the alloy amounted to 1.98±0.54 μm and was approximately two-three-fold higher than that of the deposits. Among the studied coatings, EN layer has the lowest roughness varying from 0.75 ± 0.20 μm to 0.82 ± 0.27 μm for sets 2 and 3, respectively, against the maximum R_a value of 1.22 ± 0.47 μm for a silver deposit (Table 1). The Vickers microhardness test of the outer surface of the samples demonstrates that an EN deposit has the highest hardness of ≈5 GPa among the studied coatings, which is five times higher than that of the substrate more than an order of magnitude greater than this value for silver coating (0.3 GPa) and (Table 1).

Under the assumption that the EN layer consists of Ni-P binary alloy only, the average phosphorus concentration obtained by EDS analysis (10 measurements) amounted to about 9.7±1.5%P. As an example, chemical composition in the points 1-5 of EN and EDN deposits and substrate (Fig. 1) is presented in Table 2.

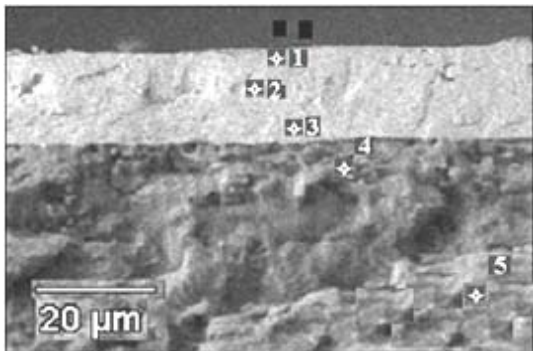

Fig. 1. The SEM microphotograph of the cross-sections of coated samples showing a two-layer Ni-based deposit (set 4) with the points corresponding to the EDS data presented in Table 2.

X-ray diffraction analysis of an EN deposit showed two peaks of amorphous Ni-P phase at 2θ of 44.6° and about 80.6°, which confirms the data reported by Lewis and Marshal [9] corresponding to the crystallite size ≤ 1.5 nm.

Table 2. Chemical composition of the substrate and deposits (set 4) in accordance with EDS analysis in the points given in Fig. 1.

Point	Ni	P	Al	O	C
1	75.3	0	1.2	5.0	18.5
2	74.6	8.0	0.7	4.0	12.7
3	69.7	9.2	0.8	4.3	16.0
4	50.7	5.9	18.8	8.2	16.4
5	0	0	72	6.4	21.6

3.2. Tensile properties of the alloy

The tensile tests carried out on uncoated 6061-T6 aluminum alloy indicated an ultimate tensile strength (UTS) of 345±4 MPa, tensile yield stress ($TYS_{0.2\%}$) of 300±3 MPa and elongation-to-fracture (δ) of 11.9±1.1% (Table 3).

Table 3. Tensile mechanical properties of the reference and coated alloy.

Set No.	**UTS, MPa**	**$TYS_{0.2\%}$, MPa**	**δ, %**
1	345±4	300±3	11.9±1.1
2	324±6	272±4	10.1±1.6
3	333±3	300±5	6.0±2.1
4	331±3	284±6	10.2±1.2
5	323±5	299±4	6.8±1.0
6	322±4	281±6	10.0±2.0
7	316±8	306±7	6.2±1.0

All sets of coated aluminum alloy may be divided into two groups in accordance with the deposit thickness and results of tensile tests: a group A including the alloy coated with a 12-μm-thick inner EN layer (sets 2, 4 and 6) and a group B including the samples coated with a 26-μm-thick inner EN layer (sets 3, 5 and 7). After the electroless nickel plating, the UTS of the samples of sets 2 and 3 decreased from 345±4 MPa to 324±6 MPa and to 333±3 MPa for 12-μm-thick and 26-μm-thick layers, respectively, whereas the $TYS_{0.2\%}$ decreased up to 272±4 MPa only for the first coated system. In general, the maximum strength for both groups is 4% -8% lower than in the substrate, and TYS for group A is also 6% - 9 % lower than that of the substrate. The yield properties of samples related to group B, in which the inner EN layer is two-fold greater than in group A, were practically the same as in an uncoated alloy. Elongation (δ) for the samples of the group A is varied in the range from 10.0 ± 2.0 % to 10.2 ± 1.2% and remains almost unchanged for an uncoated alloy, for which $\delta = 11.9$ (Table 3, sets 2, 4 and 6). However, the samples of the group B with a greater deposit thickness showed two-fold decrease in elongation as compared to the uncoated alloy (Table 3, sets 3, 5 and 7). In general, coated samples related to the group A are more ductile than the sample from the group B, in which the thickness of deposited layers is more than two-fold greater (Tables 1, 3).

3.3. Fatigue properties of the alloy

A typical presentation of low-cycle fatigue test results is satisfactorily described by a well-known Coffin-Manson relation [10, 11]: $\Delta\varepsilon_{pl} = \varepsilon_f^{'} N^{-c}$, where $\Delta\varepsilon_{pl}$ is the plastic strain amplitude, $\varepsilon_f^{'}$ is approximately equal to the true fracture strain and is called fatigue ductility coefficient, N is the number of cycles to failure, 'c' is so-called fatigue ductility exponent, which, as a rule, varies for metals in a relatively narrow interval (0.4 – 0.6). The exponent c reflects the ductility and hardening of metal under cycling strain. The importance of the Coffin-Manson equation consists in the possibility of its use for predicting fatigue behavior when the two parameters have been measured.

The $\Delta\varepsilon_{pl} - N$ diagrams for the substrate 6061 and coated alloy are presented in Fig. 2. The fatigue life of 6061 substrate dramatically decreases with an increase in the plastic strain amplitude $\Delta\varepsilon_p$ from 0.003 to 0.010.

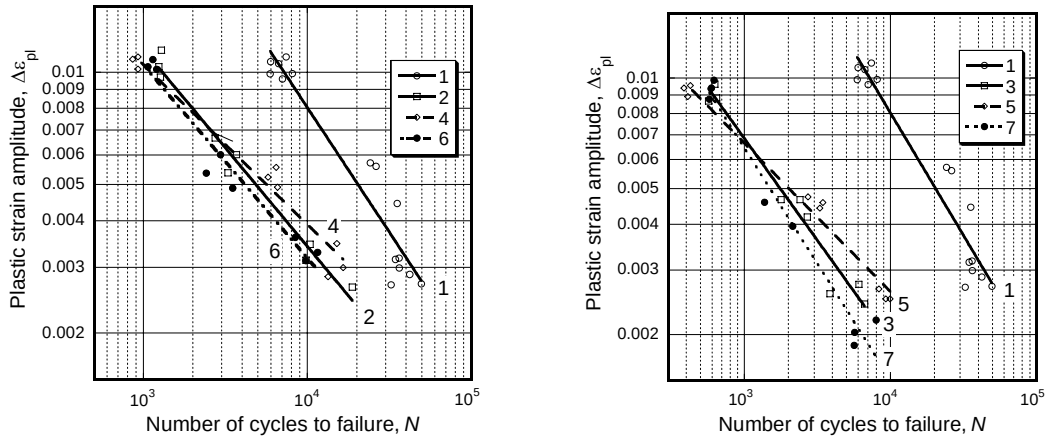

(a) (b)

Fig. 2. Fatigue life of Al 6061-T6 substrate (1) as compared to that for the 6061-T6 alloy coated with a single layer (2, 3); two-layer (4, 5) and three-layer (6, 7) coatings depending on plastic strain amplitude. The curve numbers correspond to the set numbers mentioned in Table 1; the thickness of EN layer adjacent to the substrate, μm: 12(a) and 26 (b).

It was found that the fatigue ductility exponent for an uncoated alloy amounted to 0.667, while for plated samples of sets 2 -7, it varied from 0.404 to 0.603. Fatigue ductility coefficient for the Al substrate amounted to 3.751 and was around an order of value greater than that for coated systems represented by sets 2 -7, where ε_f' values varied from 0.108 to 0.500 (Table 4). Thus, both fatigue and tensile tests showed a drastic deterioration of plasticity for coated 6061 alloy as compared to the substrate.

As it can be seen from Fig. 2, deposition of a single electroless 12-μm-thick layer and, especially, a 26-μm-thick Ni layer significantly shortens the lifetime of the system 6061-T6/ EN as compared to the uncoated alloy. The mean lifetime of the alloy plated with 12-μm and 26-μm-thick EN layers amounted to 13,008 and 5.535 cycles, respectively, as compared to 45,849 cycles for the substrate at the smallest plastic strain amplitude of 0.003 (Table 5).

Table 4. Coefficients of fitting equations $\Delta\varepsilon_{pl} = \varepsilon'_f N^{-c}$

Set No.	ε_f'	c	Correlation coefficient r^2
1	3.751	0.667	0.939
2	0.440	0.528	0.968
3	0.316	0.555	0.970
4	0.201	0.428	0.982
5	0.108	0.404	0.986
6	0.372	0.517	0.960
7	0.500	0.630	0.974

Therefore, the relative lifetime N_{fc}/N_{fs} of these coated systems (sets 2 and 3) amounted only to 0.28 and 0.12 as compared to the substrate, where N_{fc} and N_{fs} are the numbers of cycles to failure for the coated alloy and the substrate, respectively. An increase in the plastic strain up to 0.005 and 0.010 leads to an additional degradation of fatigue properties both for 12-μm- and 26-μm-thick EN deposits.

Table 5. Mean and relative lifetimes (N_f , N_{fc}/N_{fs}) and the standard deviation of results (SD) for uncoated (1) and coated Al alloy (2-7) as a function of plastic strain amplitude $\Delta\varepsilon_{pl}$

$\Delta\varepsilon_{pl}$	0.003			0.005			0.010		
Set No.	N_f	SD	N_{fc}/N_{fs}	N_f	SD	N_{fc}/N_{fs}	N_f	SD	N_{fc}/N_{fs}
1	45,849	5,223	1	28,612	5,969	1	6,855	843	1
2	13,008	1,120	0.28	3,234	473	0.11	1,266	23	0.18
3	5,535	1,476	0.12	2,299	467	0.08	614	41	0.09
4	15,014	1,592	0.33	6,263	440	0.22	902	37	0.13
5	9,197	831	0.20	3,150	376	0.11	407	21	0.06
6	9,920	1,546	0.22	2,957	546	0.10	1,137	71	0.17
7	6,427	1,338	0.14	1,757	541	0.06	596	21	0.09

The second 4 μm-thick EDN-layer electroplated on the electroless Ni layer (sets 4 and 5) insignificantly reduced the fatigue life of the coated alloy at a relatively high plastic strain of 0.010, probably, due to the 'thickness effect': the thicker the coating, the greater lifetime reduction (Table 5, Fig. 2). However, at medium and low strain levels corresponding to the number of cycles more than 10^3, a marked improvement of fatigue properties was found. For example, at $\Delta\varepsilon_{pl}$ = 0.003, lifetime of sets 4 and 5 amounted to 15,014 and 9,197 cycles, respectively, as compared to 13,008 and 5.535 cycles for sets 2 and 3, which were not electroplated with EDN (Table 5). Especially strong influence of EDN deposit improving the fatigue properties of a two-layered system was found for set 5 at medium and low plastic strains (Fig. 2, Table 5).

All fatigue curves obtained for a coated alloy are located on the left of the $\varepsilon - N$ diagram for the substrate, which demonstrates a reduction in the cyclic longevity as a result of embrittlement of the system by EN layer (Fig. 2). It is well-known that tensile strength and hardness of an EN deposit (7% - 9%P) are almost twice higher than that of EDN: UTS amounts to about 0.95 GPa and 0.51 GPa; HV - 4.7 GPa and 2.0 GPa respectively, [5, 11]. Ductility of EN is, accordingly, much less than that of EDN: elongation-to-fracture is usually equal to 1% vs. 5-30% for the coating electrodeposited in a sulfamate bath [11].

In accordance to our data, the hardness value of electroplated nickel is about 1.9 GPa vs. 5.1 GPa for electroless nickel (Table 1). It seems that at relatively minor plastic strain amplitudes, a much more ductile electroplated Ni-layer prevents crack formation on the outer surface of the coated alloy and, probably, in the interface between Ni layers. Of course, at high strains, EDN layer does not prevent the intensive cracking observed already after the first cycle contrary to that for a lower plastic strain (Fig. 5). Cracking after the 1st cycle was found at $\Delta\varepsilon_{pl}$ = 0.010 both in the outer EDN layer and in the inner 12-μm-thick EN deposit (Figs. 5b, 6a**).**

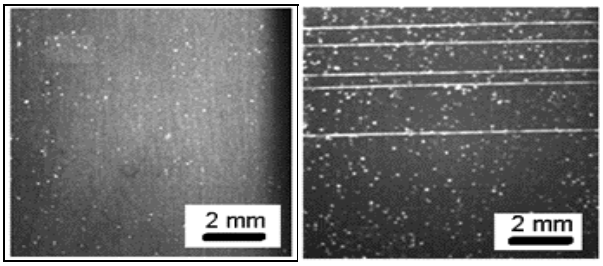

Fig. 5. The view of an EDN layer on the lateral sample surface (set 4) after one cycle at plastic strain amplitude of 0.003 (a) and 0.010 (b).

The dynamics of the crack propagation in samples coated with two-Ni-layers (set 4) at the medium plastic strain of 0.005 is illustrated in the pictures corresponding to 0.2; 0.4 and 0.8 of fatigue life (Figs. 6b, 6c and 6d). It can be clearly seen that cracking occurs, mainly, at the interface between the inner electroless nickel layer and the Al substrate. As expected, the cracks nucleated near various heterogeneities of the surface, e.g., hillock-type defects (Fig. 6a, 6b), pores (Fig. 7c), etc.

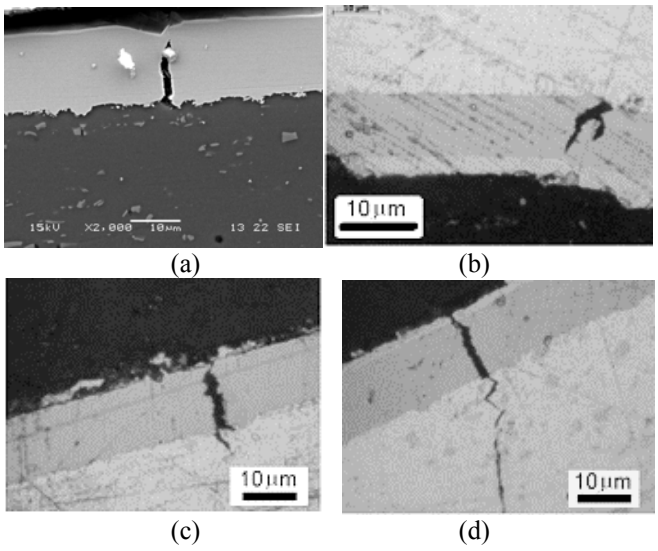

Fig. 6. SEM (a) and optical (b, c, d) micrographs of cracks in samples of set 4 originated at the interface between electroless nickel layer and Al substrate at $\Delta\varepsilon_{pl}$: 0.010 (a) and 0.005 (b, c, d). Number of cycles: one (a); 1253 or 0.2N_f (b), 2505 or 0.4N_f (c) and 5010 or 0.8N_f (d).

In the uncoated alloy, the final fatigue fracture, as can be distinctly seen in Fig. 7a, has been originated at such surface defect as a pit 'A'. The fracture process starting from a pit was dominated by the propagation of a single crack with the directions marked by arrows. In contrast to high-cycle fatigue fracture patterns, the LCF fracture surface can include the striations in the area of an initial rupture close to the sample surface [13] as demonstrated in Fig. 7b. An origin of the fracture 'A', a secondary crack 'B' and striations 'S' in a three-layered coated sample (set 6) are shown in Figures 7b, 7c and 7d. In a tilted sample of set 3, very fine striations 'S1' in EN deposit and striations 'S2' in the substrate were observed (Fig. 8).

In contrast to results reported in the literature for aluminum alloys coated with electroless nickel in high-cycle fatigue range ($N>10^4$), the lifetime of the Al alloy coated with the same deposit is greatly shortened as compared to that of the substrate in low-cycle fatigue tests ($N<10^4$). For instance, after depositing 12-μm- and 26-μm-thick layers of electroless nickel at maximum plastic strain of 0.003, it decreased by 72% and 88%, respectively, as compared to uncoated alloy. Since coated components used in engineering applications may include different stress concentrators, a designer should always take into account the possibility of occurrence of local plastic deformation.

Therefore, even relatively low-frequency strain cycling, e.g., during start and stop operations, may cause the low-cycle fatigue failure.

Thus, it was found that the thickness and type of coating have a pronounced impact on the ductility and fatigue lifetime of the alloy.

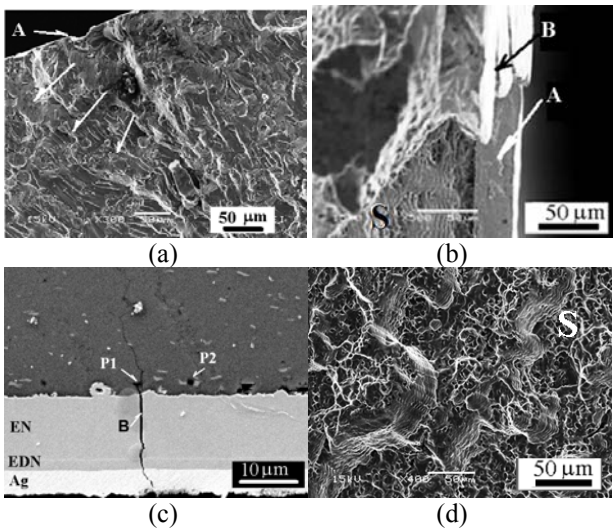

Fig. 7. Crack initiation sites 'A' on the fracture surface of uncoated (a) and three-layer-coated alloy (b-d, set 6) with secondary cracks 'B' (b, c) and striations 'S' close to the alloy surface (b) and in the texturized grains in the bulk of the sample (d).

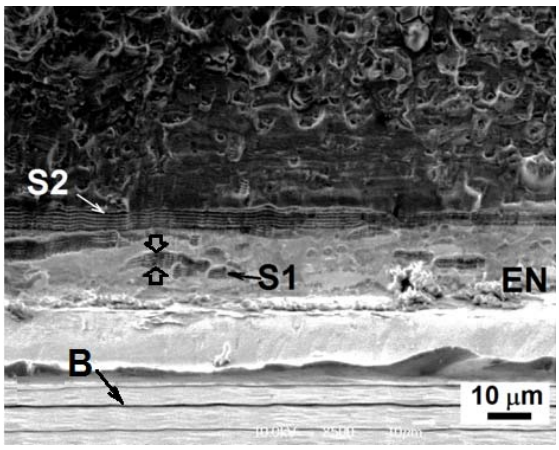

Fig. 8. SEM micrographs of the fracture surfaces of tilted sample (set 3) with striations in EN layer (S1) and in substrate (S2) and the secondary crack 'B' ($\Delta\varepsilon_{pl}$ = 0.003). Broad arrows bracket 6 striations.

4. Conclusions

Low-cycle fatigue of 6061-T6 Al alloy coated with nickel, gold and silver was studied in a pure bending strain-controlled mode, which is more complicated than the usually reported uniaxial push-pull loading mode. The tensile and fatigue properties of the alloy coated with multi-layered deposits depend, first of all, on the thickness of the inner hard electroless nickel layer that drastically decreases the ductility of the system.

It was found that in contrast to results of high-cycle fatigue of aluminum alloys coated with electroless nickel, the lifetime of the Al alloy plated with EN deposit in LCF range is greatly shortened as compared to that of the substrate. For instance, lifetime decreases by 72% and 88% as compared to uncoated alloy after depositing 12-μm- and 26-μm-thick layers of electroless nickel at maximum plastic strain of 0.003, respectively.

Incipient cracks were revealed, first of all, in the electroless nickel layer and in the substrate close to its surface. Electroplating by the second ductile Ni layer increases the lifetime of the alloy in comparison with that coated only by the electroless Ni layer.

References

[1] M. Kutz, Protective coatings for aluminum alloys, Handbook of Environmental Degradation of Materials, Ed. M. Kutz, 2nd ed., Elsevier (2012).
[2] E. Cirik, K. Genel, Surf Coat Technol **202**, 5190 (2008).
[3] J. A. M. Camargo, H. J. Cornelis, V. M. O. H. Cioffi, M. Y. P. Costa, Surf Coat Technol **201,** 9448 (2007).
[4] C. J. Villalobos-Gutierrez, G. E. Gedler-Chacon, J. G. La Barbera-Sosa, A. Pineiro, M.H. Staia, J. Lesage, D. Chicot, G. Mesmacque, E.S. Puchi-Cabrera. Surf Coat Technol **202,** 4572 (2008).
[5] D. W. Baudrand, Electroless Nickel Plating, Surface Engineering, ASM Handbook, Vol. 5, ASM International, Materials Park, OH 44073, 1994, pp. 954.
[6] E.S. Puchi-Cabrera, C. Villalobos-Gutierrez, I. Irausquın, J. La Barbera-Sosa, G. Mesmacque, Int J Fatig **28,** 1854 (2006).
[7] B. Lonyuk, I. Apachitei and J. Duszczyk, Scripta Materialia **57,** 783 (2007).
[8] Ya.B. Unigovski, G. Lothongkum, E.M. Gutman, D. Alush, R. Cohen, Corr Sci **51**(12), 3014 (2009).
[9] D.B. Lewis, G.W. Marshal, Surf Coat Technol **78** (1–3), 150 (1996).
[10] L.F.Coffin, Transactions of AIME **76**, 931 (1954).
[11] S.S. Manson, NASA report 1170,, Lewis Flight Propulsion Laboratory, Cleveland, 1954.
[12] G. Di Bari, Surface Engineering, ASM Handbook, Vol. 5, publ. ASM International, Materials Park, OH 44073, 1994, pp. 742-765.
[13] SEM/TEM Fractography Handbook, Publ. Metals and Ceramic Information Center, Columbus, USA, 1975.

* Corresponding author: yakovun@exchange.bgu.ac.il